Estimating vertical and horizontal resistivity of the overburden and the reservoir for the Alvheim – Boa field.

Folke Engelmark and Johan Mattsson, PGS*

Summary

Towed streamer EM data was acquired in October 2012 over the Alvheim – Boa Field located in the Norwegian sector of the North Sea. It is a challenging target consisting of a medium sized oil & gas field exhibiting an average transverse resistance located at 2,100 m below mudline. A depth model was defined for both the overburden and the reservoir interval based on an available well log, and the data was inverted as a series of 1D inversions for all common mid-points along two survey lines to form 2D resistivity sections. Both the vertical and horizontal resistivities were inverted for by minimizing the difference in the frequency responses between forward modeled data and the acquired towed streamer EM field data. Hence, the inversions were done with only a ten layer depth model as background information plus one value for the under-burden. The reservoir interval itself displays high anisotropy as expected since the reservoir is a turbidite. It consists of high resistivity hydrocarbon-charged sands inter-bedded with low resistivity shales giving rise to an effective anisotropy ratio of around 5, whereas the proximal overburden layer exhibits an anisotropy of 2.6. When the anisotropy can be evaluated, the net-to-gross can be estimated facilitating a much improved quantitative estimate of the hydrocarbons in place. Further, when an anisotropic reservoir is located in proximity to or directly on top of basement it can be detected by means of the anisotropy alone. The basement is likely to be isotropic or even display inverse anisotropy due to vertical fractures being more abundant, wider and hence also better conducting than tight horizontal fractures.

Introduction

Controlled source electro-magnetic (CSEM) marine methods have traditionally been node-based systems, where the receivers are placed as autonomous recording stations on the seafloor in a very sparse line or areal pattern. The source is then towed close to the seafloor emitting a constant source signal, which is typically a square-wave.

The first available towed streamer EM system was tested in its final form in October 2012. The similarities to seismic acquisition are obvious, and the advantages are many including acquisition speed at 4-5 knots, fixed source - receiver geometry, dense common mid-point (cmp) sampling, real-time quality control and on-board processing facilitating a quick-look at the transverse resistance of the reservoir. The Alvheim – Boa reservoir, known as the Alvheim sandstone, is a challenging target due to average size and a depth of burial at 2,100 m below mudline. The reservoir is a turbidite. They are notoriously difficult to evaluate, even in wireline log data, and often show a rather low net-to-gross (N/G). A weak but consistent anomaly is seen in the towed streamer EM data next to the depocenter, and most significant is that a series of 1D cmp inversions along the survey lines results in a strong anisotropy to be assigned to the reservoir, in order for the inversion to converge properly. The anisotropy is not intrinsic to any lithology but arises as an effective anisotropy from the nature of turbidite reservoirs, where the highly resistive hydrocarbon-charged sands are inter-bedded with low resistivity shales.

The towed streamer EM acquisition method

The layout of the acquisition system is shown in Figure 1 below. The bi-pole source is 800 m long and towed at 10 m depth. The source-signal sequence is 120 s long with the source active the first 100 s followed by 20 s of no signal that is used for background noise estimation and noise reduction processing. The source runs at 1,500 amperes and the source signal is user selectable. Our current favorite is the so called Optimized Repeated Sequence (ORS). It can be viewed as a square-wave with twice the density of the discrete harmonics seen in a regular square-wave. The EM streamer has effectively 26 offsets varying from 0 – 7,700 m and it is towed at a nominal depth of 100 m. The maximum water depth is 400 m. Greater water depths are acceptable if the target is large, shallow below mudline, and highly resistive. The towing speed is 4 – 5 knots.

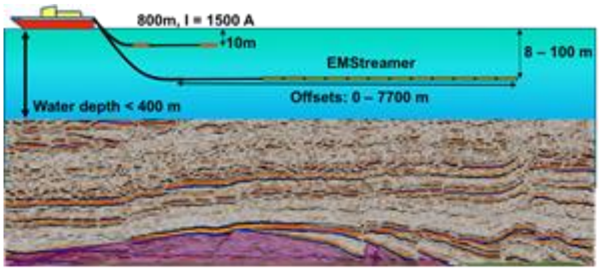

Figure 1: The layout of the acquisition system is similar to 2D seismic. The 800 m long bi-pole source is towed at 10 m emitting a 1,500 A source signal. The streamer has offsets from 0 - 7,700 m and it is towed at a nominal depth of 100 m. The towing speed is 4 – 5 knots.

Noise reduction is implemented in a number of different ways as described by Mattsson et al (2012). Stochastic

DOI http://dx.doi.org/10.1190/segam2013-0764.1

noise is attenuated by two methods. First the dense sampling both within the streamer and along the survey lines facilitates noise reduction by stacking which improves signal-to-noise by a factor $N^{1/2}$, where N is the number of stacked signals. The second method is the so-called low rank approximation based on singular value decomposition. It takes advantage of the fact that the signal occupies only discrete frequencies, whereas the stochastic noise is spread throughout the spectrum. By identifying the discrete signal frequencies, all noise between these frequencies can be removed.

The survey lines and the Alvheim – Boa field

The two survey lines strike in the NNE direction in parallel over the Boa reservoir as seen in Figure 2. The locations of the lines are suboptimal due to permit constraints and existing infrastructure in the area, but they are traversing very close to the Boa depocenter as mapped from the seismic data and seen in warm colors to the left of the survey lines. Immediately to the right of these, there is a reference line showing the common distance for both lines from an arbitrary point outside the reservoir. The direction of sailing is also shown as South to North for line 201 and from North to South for line 202.

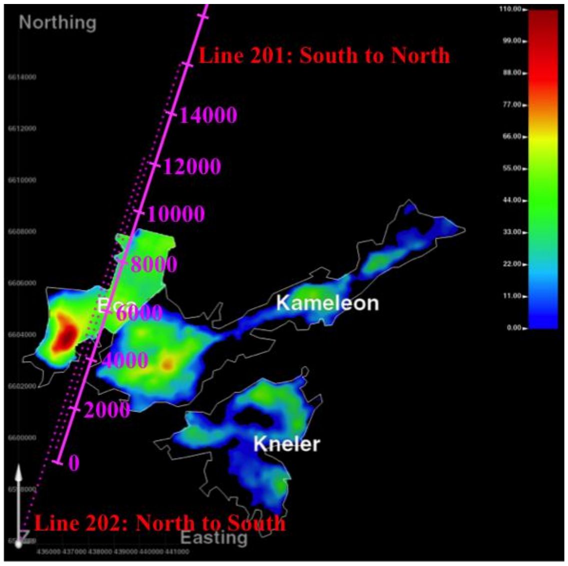

Figure 2: The Alvheim – Boa oil and gas field. The two survey lines are shown as magenta dotted lines. The Boa depocenter mapped from seismic is seen as the red anomaly immediately to the left of the lines. The color scale shows the reservoir thickness in meters. The solid magenta line is a reference line in meters common to both survey lines. Line 201 was shot from South to North, and Line 202 from North to South.

Figure 3 below shows the deep induction resistivity log (red) from well 1 in the field. The green curve is the estimated resistivity based on a transform from velocity to resistivity for shales as described in Engelmark (2010). The two yellow fields highlight the Utsira sand (100 – 710 m) and the Heimdal sandstone, which is the Alvheim – Boa reservoir (2040 – 2320 m). The resistivity log, in this case a deep induction log, measures horizontal resistivity. Modern tri-axial tools that simultaneously measure vertical and horizontal resistivity have been introduced, but are still rarely used.

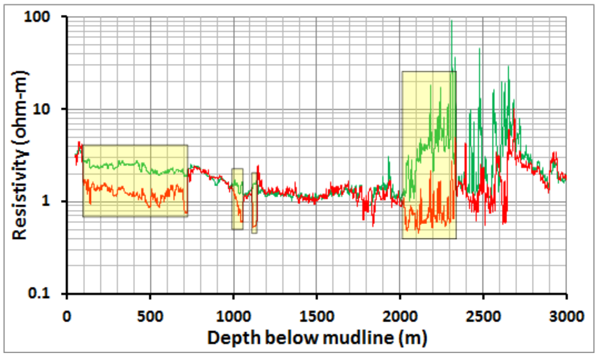

Figure 3: Resistivity log (red) from a well penetrating the Boa reservoir (2,020 – 2,330 m below mudline) outside the hydrocarbon charged volume. The green curve is a shale-resistivity model based on the sonic log. Major sands are highlighted in yellow where the shale model deviates from the log as expected. The Utsira sand (shallow) and Heimdal reservoir (deep) are highlighted in yellow.

Resistivity estimation

The vertical and horizontal resistivities below the mud-line were estimated along the two survey lines by means of 1D multi-trace anisotropic inversion. The 1D inversions were done individually for each common-mid-point (cmp) and then stitched together to form a 2D resistivity section along the survey lines. The inversion is formulated as a minimization problem using a trust-region-reflective algorithm based on the interior-reflective Newton method, described by Coleman and Li (1994, 1996). Each iteration involves the approximate solution of a large linear system using the method of preconditioned conjugate gradients. The objective function is defined as the L2-norm of the weighted differences between measured and modeled frequency response data. The associated frequency response uncertainties are used in the weights to down-scale the noisy data.

For both survey lines an eleven layer model has been estimated at each cmp. In this case, the seawater is approximated as one layer with a resistivity of 0.259 ohm-m taken from a conductivity, temperature & depth (CTD) measurements. The water depth is estimated from echo sounder measurements on board the vessel. The water depth varies in the model from 110 m in the north of the

DOI http://dx.doi.org/10.1190/segam2013-0764.1

lines to 125 m in the south area. The subsea sediments were then divided into ten layers where the first two represent the overburden stretching from seafloor to the base of the Utsira sand for the first layer, and from the base of Utsira to the top of the Heimdal sandstone for the deeper layer.

The Heimdal reservoir, also mapped in depth and thickness according to the well log, was then discretized into seven equally thick layers of 70 m followed by a half-space of under-burden. All subsurface layer thicknesses were kept fixed and equal for all cmps during the inversion and it is only the vertical and horizontal resistivities for each layer that are inverted for. Hence, in total ten vertical and ten horizontal resistivity values are estimated through inversion at each cmp. Six frequencies and eight offsets were used for all the inversions as listed below:

- Frequencies: 0.05, 0.015, 0.20, 0.25, 0.30, and 0.75 Hz.
- Offsets: 3550, 4000, 4450, 5050, 5650, 6250, 6850, and 7450 m.

Even though shorter offsets are used in the streamer, they are neglected in the data going into the inversion. The reason is that a more finely resolved structure based on seismic data is needed to capture the variations in these short offsets. However, to characterize the deeper anomaly region and to roughly estimate the overburden, the set of offsets from 3550 – 7450 m is sufficient. The selected frequency range from the ORS source sequence mentioned above is chosen to be sensitive to the anomaly region but also sufficient to be able to estimate both the vertical and horizontal resistivities in the two layer thick overburden model.

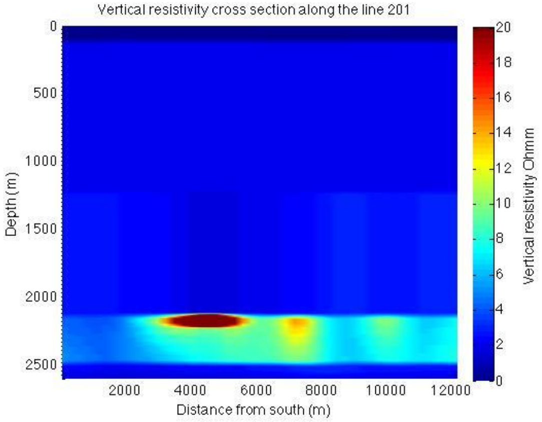

Figure 4: The estimated vertical resistivity for Line 201.

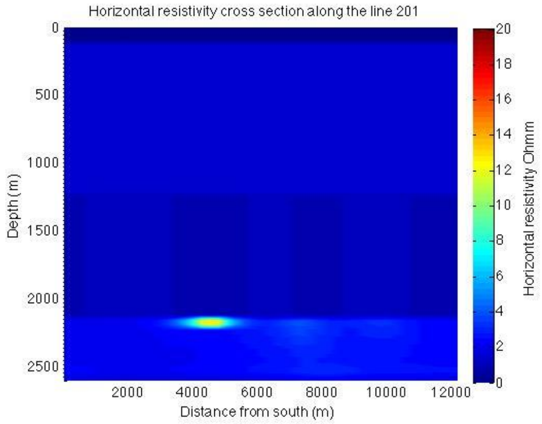

Figure 5: The estimated horizontal resistivity for Line 201.

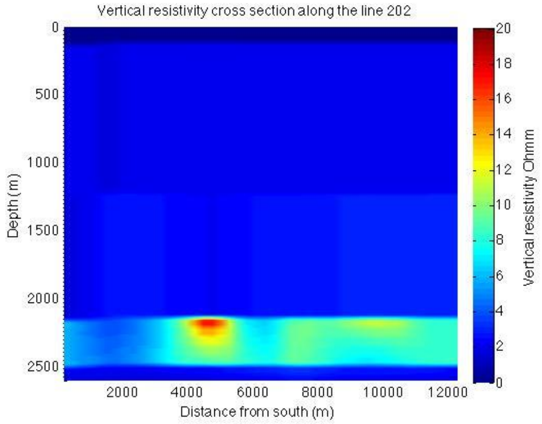

Figure 6: The estimated vertical resistivity for Line 202.

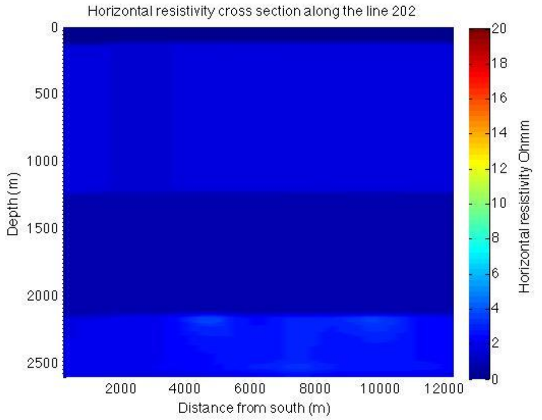

Figure 7: The estimated horizontal resistivity for Line 202

The resulting vertical and horizontal resistivity cross sections are shown in Figures 4 & 5 respectively for Line 201 and in Figures 6 & 7 for Line 202. Line 201 is somewhat closer to the depocenter, hence also showing somewhat stronger anomalies. It can be concluded that the resistivity increase occurs at roughly the same lateral position and depth for both survey lines.

The positions of the anomalies also coincide well with the maximum seismic amplitude according to Figure 2. The horizontal resistivity is also seen to increase where the maximum vertical resistivity occurs. Hence, even in a rather thin reservoir layer, there is still some sensitivity to the horizontal component in the inline data. Further, the thicknesses of the anomalies in the cross-sections agree well with expected values. The vertical resistivity is the volumetrically weighted arithmetic average of the oil/gas charged sand and shale resistivities, and the horizontal resistivity is the volumetrically weighted harmonic average of the two lithologies. The peak vertical resistivity along line 201 is around 50 ohm-m, whereas the horizontal resistivity increases to 10 ohm-m as shown in Figure 8 below. Assuming the average resistivity for the shales is 1.1 ohm-m, then the resistivity of the sands must be 55 ohm-m resulting in a N/G of 0.91. A similar argument for line 202, located more distant from the depocenter than line 201, results in shale and sand resistivities of 1.1 and 24 ohm-m respectively and a N/G of 0.82.

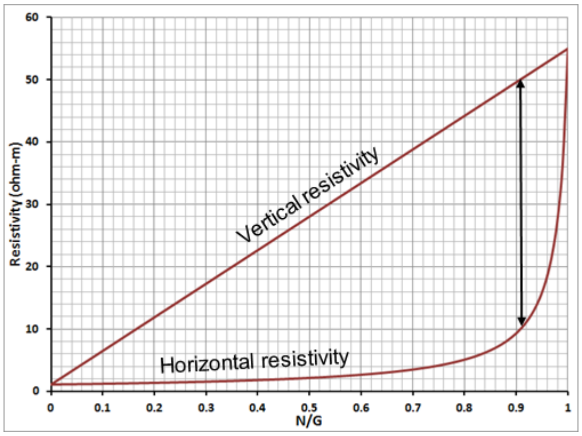

Figure 8: The vertical and horizontal resistivities as a function of N/G for Line 201. At a N/G of 0.91 the two resistivities are in agreement with the inverted data.

The relative difference, or misfit, between the measured and modeled frequency responses after inversion was plotted as a function of offset and frequency for both the amplitude and the phase. The result for the relative amplitude difference is largely below 4%, as shown in Figure 9, and the phase difference is below 2 % as seen in Figure 10. These values are at similar levels as the residual noise in the field data after processing.

Conclusions

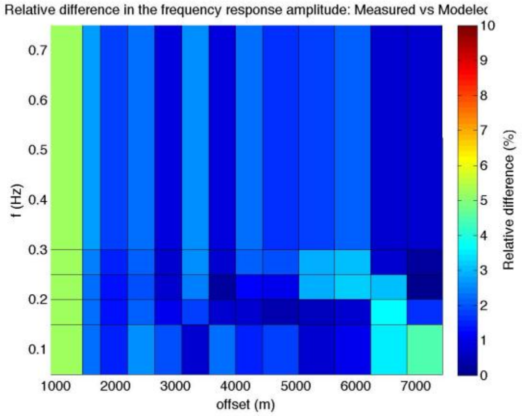

Figure 9: Examples of the difference between measured and modeled frequency amplitude response.

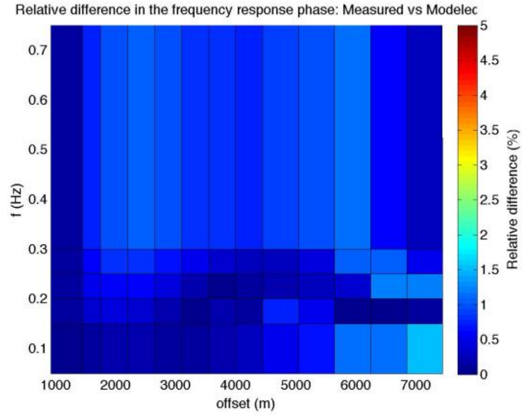

Figure 10: Examples of the difference between measured and modeled frequency phase response.

The Alvheim – Boa Field is a challenging target due to the combination of depth below mudline (2,100 m), limited lateral extension of the reservoir's depocenter (~2,000 m) and a low transverse resistance of the reservoir. The survey results and the inverted data show that we can use a data driven inversion to estimate both vertical and horizontal resistivity of the overburden as well as in the reservoir. Further, the reservoir is found to be anisotropic which in principle makes it possible to estimate net-to-gross (N/G) facilitating a better estimate of the hydrocarbons in place.

Towed streamer EM data can hence be used to evaluate both the vertical and horizontal resistivity, facilitating an estimate of N/G resulting in improved estimates of hydrocarbon volumes in place. It is especially important when evaluating reservoirs close to or directly on top of the basement, a case that has been considered difficult for EM to resolve. The reservoir interval will show anisotropy due to a limited N/G, for example as in this case a turbidite sand, whereas the basement is likely to be isotropic or having a reversed anisotropy due to vertical fractures being more frequent and more conductive than horizontal fractures. The charged reservoir can then be convincingly detected based on anisotropy alone.

DOI http://dx.doi.org/10.1190/segam2013-0764.1

http://dx.doi.org/10.1190/segam2013-0764.1

EDITED REFERENCES

REFERENCES

Coleman, T. F., and Y. Li, 1994, On the convergence of reflective newton methods for large-scale nonlinear minimization subject to bounds: Mathematical Programming, **67**, no. 2, 189–224. http://dx.doi.org/10.1007/BF01582221.

Coleman, T. F., and Y. Li, 1996, An interior, trust region approach for nonlinear minimization subject to bounds: SIAM Journal on Optimization, **6**, no. 2, 418–445, http://dx.doi.org/10.1137/0806023.

Engelmark, F., 2010, Velocity to resistivity transform via porosity: Presented at the 80th Annual International Meeting, SEG.

Mattsson, J., P. Lindqvist, R. Juhasz, and E. Björnemo, 2012, Noise reduction and error analysis for a towed EM system: 82nd Annual International Meeting, SEG, Expanded Abstracts, 1–5.

DOI http://dx.doi.org/10.1190/segam2013-0764.1